THE ROYAL SOCIETY

*Received* 12 April 2002
*Accepted* 9 June 2002
*Published online* 28 August 2002

# Decorrelation control by the cerebellum achieves oculomotor plant compensation in simulated vestibulo-ocular reflex

**Paul Dean*, John Porrill and James V. Stone**

*Department of Psychology, University of Sheffield, Western Bank, Sheffield S10 2TP, UK*

We introduce decorrelation control as a candidate algorithm for the cerebellar microcircuit and demonstrate its utility for oculomotor plant compensation in a linear model of the vestibulo-ocular reflex (VOR). Using an adaptive-filter representation of cerebellar cortex and an anti-Hebbian learning rule, the algorithm learnt to compensate for the oculomotor plant by minimizing correlations between a predictor variable (eye-movement command) and a target variable (retinal slip), without requiring a motor-error signal. Because it also provides an estimate of the unpredicted component of the target variable, decorrelation control can simplify both motor coordination and sensory acquisition. It thus unifies motor and sensory cerebellar functions.

**Keywords:** oculomotor; cerebellum; vestibuloocular reflex; motor learning; integrator

## 1. INTRODUCTION

The uniform microstructure of cerebellar cortex indicates the existence of a basic cerebellar algorithm, applicable in many different contexts (Ito 1984). This algorithm has proved difficult to identify, not least because the functions of the cerebellum appear to be a disconcerting blend of the sensory and motor. Although the classical signs of cerebellar dysfunction relate to motor control, comparative studies in a wide range of vertebrates suggest that the expansion of cerebellar regions is associated with complexity of sensory processing (Paulin 1993) and a variety of experimental results have indicated a role for the cerebellum in the acquisition and prediction of sensory data (e.g. Blakemore *et al.* 2000; Hartmann & Bower 2001; Nixon & Passingham 2001). We propose here a candidate algorithm for the cerebellum, which we term decorrelation control, that offers the possibility of reconciling sensory and motor views of cerebellar function.

Decorrelation control can be considered a development of adaptive interference–cancellation (Widrow & Stearns 1985). In generic interference–cancellation (figure 1*a*), a signal of interest $u$ is corrupted by additive interference $n$ to form what is termed here the target variable, $u + n$. Predictor variables $p$ carry versions of the interference $n$, distorted in unknown ways. The goal of the adaptive processor (labelled 'decorrelator' in figure 1*a*) is to produce an output $\hat{n}$ that approximates the interference, so that when $\hat{n}$ is subtracted from the target variable, the resultant output of the system $\hat{u}$ $(= u + n - \hat{n})$ approximates the original signal of interest $u$. The output $\hat{u}$ is also used as a training signal and the adaptive processor changes as long as there remains any correlation between the training signal and the predictor variables, because such a correlation means that there is still predictable interference present. Thus, even though the version of the interference carried by the predictor variables was distorted in ways unknown to the adaptive processor, an appropriate decorrelation algorithm will eventually produce a system output that is uncorrelated with the predictor variables. This system output is an estimate of the uncontaminated signal of interest. Decorrelating predictor and target variables is in effect minimizing the mean-squared error of the interference estimate (see Appendix A).

The relevance of adaptive interference–cancellation for understanding the cerebellar algorithm is that it is one of the functions proposed for 'cerebellar-like' structures in fish, such as the dorsal octavolateral nucleus of elasmobranchs and the teleost electrosensory lobe (e.g. Bell *et al.* 1997; Devor 2000). To map figure 1*a* onto a specific example, the signal of interest, $u$, would be the perturbations in an electric field that are produced by an external source. However, the response of the electroreceptors that detect this field are affected by the fish's own movements, $u + n$. The principal cells of a cerebellar-like structure receive the contaminated sensory input via synapses on their basal dendrites, and predictor variables, $p$, such as corollary discharge, via synapses between parallel fibres and their apical dendrites. These latter synapses are plastic and, in effect, form the adaptive processor. The signal delivered to the soma of the principal cells from their apical dendrites is the interference estimate, $\hat{n}$, but with the sign reversed so that it can be simply added to the contaminated sensory signal, $u + n - \hat{n}$, to produce the principal cell output, $\hat{u} = u + n - \hat{n}$. The principal cell output is thus an estimate $\hat{u}$, of the uncontaminated signal $u$, which is sent elsewhere in the brain, as well as being used as a training signal to alter the parallel-fibre synapses (cf. Nelson & Paulin 1995; Roberts & Bell 2000).

The development of adaptive interference–cancellation into decorrelation control is illustrated in figure 1*b*. The output of the decorrelator now acts as a motor command $m$ to alter the properties of the sensor that transmits the target variable, $u + n$. The alteration, which might for example consist of moving the sensor surface, is mediated via a set of physical processes referred to as the plant and, in effect, constitutes an estimate $\hat{n}$ of the interference $n$.

*Author for correspondence (p.dean@sheffield.ac.uk).

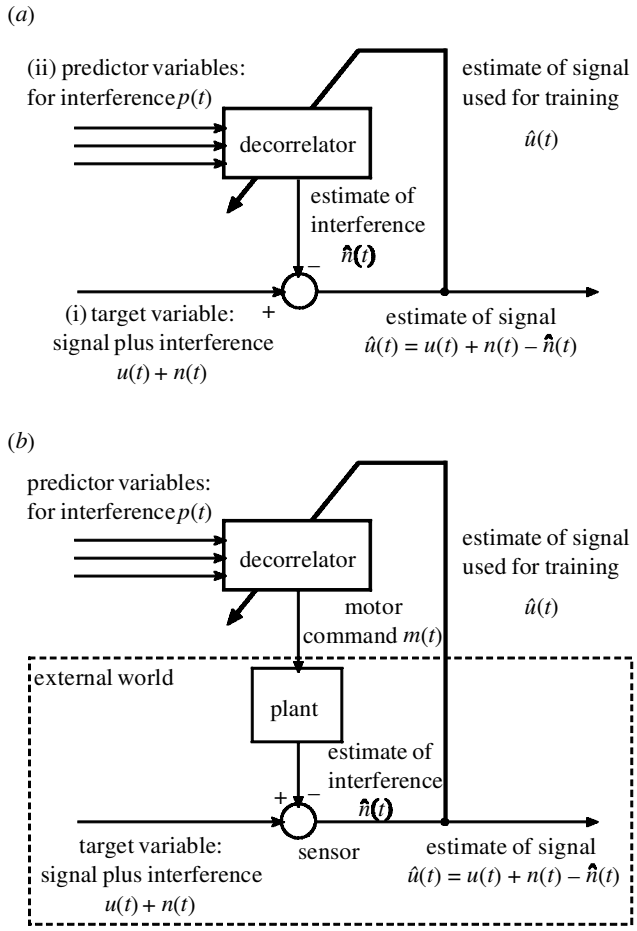


Figure 1. Relationship between adaptive interference cancellation and decorrelation control. (*a*) Adaptive interference cancellation. Inputs to the system are: (i) a target variable, which consists of an external signal of interest $u(t)$ corrupted by additive interference $n(t)$; and (ii) predictor variables $p(t)$. The task of the system is to extract an estimate of the signal of interest $\hat{u}(t)$ from the target variable. It does so by subtracting from the target variable an estimate $\hat{n}(t)$ of the interference. This estimate is constructed by the decorrelator, which learns to remove the correlations between the predictor variables and the signal estimate. (*b*) Decorrelation control. This differs from adaptive interference cancellation in that the interference estimate $\hat{n}(t)$ is now a physical adjustment of the sensor. Sensor output is no longer the target variable $u(t) + n(t)$ but the estimate $\hat{u}(t)$ of the signal of interest $u(t)$. The decorrelator must therefore learn the motor command $m(t)$ that will act on the plant to produce the appropriate interference estimate.

The new sensor output then becomes an estimate of the uncontaminated signal $\hat{u}$ $(= u + n - \hat{n})$, available for general use by the rest of the system, as well as for a training signal for the decorrelator. To map figure 1*b* onto a specific example that has long been used as a simple preparation for studying cerebellar function (e.g. Ito 1970; Lisberger 1998), one possible signal of interest is relative movement of the world as detected by image movement on the retina, $u$. The actual retinal-slip signal, $u + n$, is contaminated by interference $n$ produced by the animal's own head movements. The Purkinje cells of the cerebellar flocculus receive the contaminated sensory input via synapses from climbing fibres and predictor variables such as the vestibular response to head movement, $p$ via synapses between parallel fibres and their dendritic tree. As before, these synapses are plastic and in effect constitute the decorrelator. They drive the Purkinje cell output, which acts as a motor command, $m$ to the eye muscles, so moving the eye. The movement of the eye is, in effect, an estimate, $\hat{n}$ of the interference $n$ caused by the head movement, only with the sign reversed so that it can be simply added to the contaminated retinal-slip signal, $u + n - \hat{n}$ to produce the new retinal-slip signal, $\hat{u}$. The new signal is thus an estimate of how the world is moving, uncontaminated by head movement. If the world is in fact not moving $(u = 0)$, the result would be the abolition of retinal slip (apart from the error $n - \hat{n}$), as occurs in the vestibulo-ocular reflex (VOR).

Comparison of the two examples relevant to figure 1*a*,*b* indicates that the basic mechanism, whereby the decorrelator continues to change until correlation between predictor variables and training signal is minimized, remains the same in both adaptive interference–cancellation and decorrelation control. However, whereas the former produces an internal estimate of the signal of interest and leaves the output of the sensor unaltered, decorrelation control acts on the sensory surface to change its output until it approximates the signal of interest. As a candidate algorithm for the cerebellar microcomplex, decorrelation control therefore has the advantage of combining sensory and motor functionality.

However, the architecture illustrated in figure 1*b* also has a disadvantage, in that the decorrelator output, $m$ is no longer directly subtracted from the target variable as it was for interference cancellation (figure 1*a*). Instead, $m$ must pass though the plant $P$ in order to influence the target variable. To produce the least-squares estimate of the interference in the target variable, the system must decorrelate the predictor variables and the command (motor error) that would have produced the observed retinal slip (see Appendix A). Unfortunately, to deduce this motor error from the actual retinal-slip signal requires knowledge of the plant, which by definition is not available to the system. Decorrelation control therefore has to make do with those variables that are available, namely $p$ and $\hat{u}$, just as in adaptive interference–cancellation. But now the decorrelation learning rule is not certain to work in the general case (see Appendix A). Therefore, the important first test for decorrelation control as a candidate algorithm for cerebellar function is whether it would in fact work given the actual plant characteristics that have been observed experimentally.

We addressed this issue by examining the performance of a decorrelation controller in a model of the horizontal VOR. A highly schematic view of the neural architecture of the horizontal VOR (for a review, see Miles 1991) is shown in figure 2*a*, with the corresponding model for comparison in figure 2*b*. As illustrated in figure 2*a*, head movements are sensed by the vestibular apparatus and converted to approximate head-velocity signals. These signals are refined and passed to a brainstem path consisting of secondary vestibular neurons and ocular motor neurons. The output of the motor neurons drives the extraocular muscles that act via the mechanics of the orbital tissue to move the eye. The connectivity of the system is such that the eye moves in the opposite direction

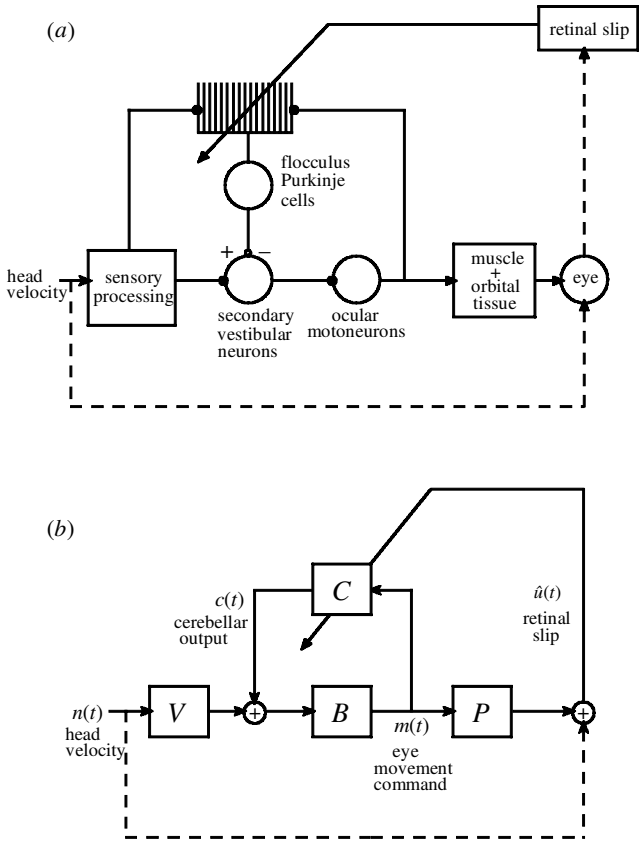


Figure 2. VOR. (*a*) Schematic neural circuitry. A processed vestibular signal related to head velocity is passed both to secondary vestibular neurons in the brainstem and to the cerebellar flocculus (in the form of mossy-fibre input). The flocculus also receives a mossy-fibre input closely related to the command sent to the eye muscles. Floccular Purkinje cells project to a subset of secondary vestibular neurons. If the command to the eye muscles does not cancel out the effects of head velocity, the eye will move relative to the world. This movement is detected as retinal slip, a copy of which is passed to the flocculus via the inferior olive as climbing-fibre input. (*b*) Linearized model. Head velocity $n(t)$ is processed by the filter $V$, then added to the output $c(t)$ of the decorrelator (cerebellar flocculus) $C$. The summed signal is then passed to a brainstem controller $B$. The output of $B$ is a motor command $m(t)$, which acts on the plant $P$. A copy of $m(t)$ is sent back to the cerebellum $C$. The effects of $m(t)$ acting on $P$ are added to the head velocity $n(t)$; the difference is detected as retinal slip $\hat{u}(t)$ and sent to $C$. Because there is no external visual signal $u(t)$ acting on the eye, the desired value of $\hat{u}(t)$ is zero. This will occur when the effects of the eye-movement command $m(t)$ acting on the plant $P$ exactly match those of the head velocity $n(t)$.

to the original head movement. The head-velocity signal is also sent as a mossy-fibre signal to the cerebellar flocculus, along with a copy of the eye-movement command. The output of the flocculus adds into the brainstem path at the level of (some) secondary vestibular neurons. Retinal-slip signals reach the flocculus as climbing-fibre inputs.

The structure of the model of the VOR used to test decorrelation control is shown in figure 2*b*. Head velocity $n(t)$ is transformed by the sensory processor $V$, which delivers a signal to brainstem neural circuitry $B$. The output $m(t)$ of $B$ is sent to the plant $P$, and so produces a command to move the eye. The combination of controller and head actions on the eye produces an eye movement with respect to the (stationary) world, namely retinal slip $\hat{u}(t)$, which is the target variable for the decorrelator $C$ (i.e. the cerebellar flocculus). The predictor variable for $C$ is the eye-movement command $m(t)$, and the output of $C$ adds to that of $V$.

It can be seen that the model in figure 2*b* is a simplified version of the architecture of figure 2*a*. The architecture was simplified because the full VOR is a complex reflex involving at least three kinds of adaptive calibration; two of these calibrations were assumed to be performed perfectly in the model.

(i) The actual signal from the semicircular canals is in part related to head acceleration and needs additional processing to produce an accurate representation of head velocity. In the model this processing is represented by $V$, which simply reproduces head velocity.

(ii) The basic gain of the VOR, which converts the head-velocity signal to the correct eye-velocity command assuming an all-viscous plant, is adaptively calibrated. However, a range of evidence indicates that this adaptation involves plasticity at both floccular and brainstem sites (see the review by Lisberger 1998). To avoid additional assumptions about the nature of the brainstem learning process, the model in figure 2*b* assumes that the brainstem process $B$ has an accurate basic gain.

The problem that remains for the decorrelator $C$ to solve is that of plant compensation. This arises because the plant $P$ (which represents the mechanical properties of both extraocular muscle and orbital tissue) has elasticity as well as viscosity. The elasticity of the plant requires an additional command signal proportional to the position of the eye, a command that for a first-order plant in one dimension is effectively an integrated eye-velocity signal (Robinson 1975). This additional signal is partly generated in the brainstem $B$ (reviewed in Fukushima & Kaneko 1995): the task of the decorrelator $C$ is therefore to fine-tune the brainstem eye-movement commands so that they accurately cancel out head movement given the particular plant properties existing at the time. The effects of floccular damage on eye-position control are consistent with a role for the flocculus in assisting the brainstem to produce accurate compensation for the plant (Zee *et al.* 1981; Optican *et al.* 1986; Fukushima & Kaneko 1995) using retinal slip as a cue (Optican & Miles 1985).

In the model illustrated in figure 2*b*, the decorrelator $C$ is represented by a generalized adaptive linear filter (Widrow & Stearns 1985; Goodwin 1998), which can be viewed as perhaps the simplest form of the basic Marr–Albus–Ito model of cerebellar cortex (Gilbert 1974; Fujita 1982*a*). The predictor variable (mossy-fibre input) is a copy of the motor command (figure 2*b*), an arrangement consistent with anatomical and electrophysiological evidence (e.g. Büttner-Ennever & Horn 1996; Belton & McCrea 2000; Nakamagoe *et al.* 2000). As shown in figure 3, the filter expands the predictor variable $m(t)$ into components $m_1(t),\ldots,m_n(t)$ (parallel-fibre signals) using appropriate basis functions (by the granule cell–Golgi cell complex). The basis functions used initially were copies

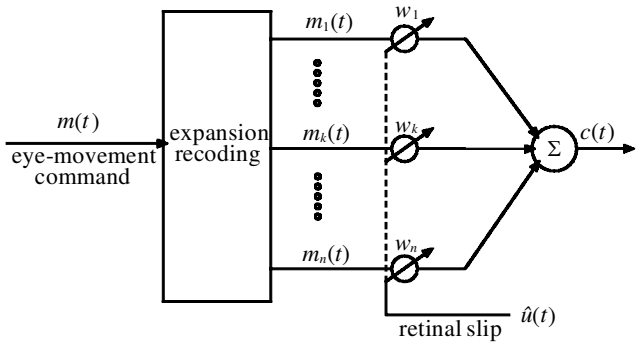


Figure 3. Structure of the decorrelator $C$ (figure 2*b*). The predictor variable $m(t)$ was recoded into components $m_1(t)$ to $m_n(t)$. Each component $m_k(t)$ was weighted by $w_k$ and then summed to produce the output $c(t)$. $w_k$ was adjusted according to the current value of the correlation between $m_k(t)$ and retinal slip $\hat{u}(t)$ (so that $w_k$ was also a function of time). Unless indicated otherwise, the recoding used in the decorrelator produced versions of the eye-movement command at increasing delays (separated by 0.02 s over 0–2 s).

of the eye-movement command at a range of delays. The estimate of the signal of interest, ($\hat{u}(t)$ in figure 2*b*) serves as a training signal (climbing-fibre input) that adjusts the component weights (parallel fibre–Purkinje cell synapses). The weighted components are summed to produce the filter output (Purkinje cell firing). The learning rule for adjusting the weights is based on Sejnowski's characterization of anti-Hebbian learning at the parallel fibre–Purkinje cell synapse as a covariance rule (Sejnowski 1977; Koch 1999). The size of the change in weight $w_k$ is proportional to the correlation between the $k$th component to the predictor variable $m_k(t)$ and the estimate $\hat{u}(t)$.

## 2. METHODS

### (a) *Basic system*

The model architecture of figure 2*b* was programmed in MATLAB. $P$, $V$, $B$ and $C$ were treated as linear processes, allowing use of functions in the control system toolbox. The characteristics of the linear processes in initial training were as follows.

(i) $V$ was a unit gain (see § 1(i) above);

(ii) $P$ was a first-order plant, with the transfer function $H_p(s)$ between eye-in-head velocity $e_h$ and motor command $m$ given by

$$H_p(s) = \frac{e_h(s)}{m(s)} = \frac{s}{s + 1/T_p}, \tag{2.1}$$

where $s$ denotes the Laplace complex frequency variable and $T_p$ is the time constant of the plant (0.2 s) (in subsequent equations with transfer functions, their argument ($s$) is omitted for simplicity).

(iii) The brainstem $B$ had the transfer function $H_b$ given by

$$H_b = G_d + \frac{G_i}{s + 1/T_i}, \tag{2.2}$$

corresponding to a brainstem controller, where $G_d$ is the direct path gain and $G_i$ is the indirect path gain. This brainstem controller has two paths: (1) a direct path which passed the head-velocity signal to the plant with the correct gain ($G_d = 1$); and (2) an indirect path in which the head-velocity signal was integrated and passed to the plant also with the correct gain ($G_i = 1/T_p = 5$). The brainstem integrator was leaky with time constant $T_i = 0.5$ s; and

(iv) the input $m(t)$ to the adaptive filter $C$ was split into 100 components; $m_1(t)$, …, $m_n(t)$, with delays between components of 0.02 s (2 s in total). $C$ was thus effectively a finite impulse response filter of length 100, with output $c(t)$ given by

$$c(t) = \sum_{i=1}^{100} w_i m(t - 0.02i), \tag{2.3}$$

where $w_i$ was the weight of component $m_i$ (figure 3). The rule for adjusting the weights was equivalent to that given in equation (A 5) in Appendix A

$$\delta w_j = -\beta \langle m_j(t).\hat{u}(t) \rangle, \tag{2.4}$$

where $\delta w_j$ was the change in the $j$th weight $w_j$ $\beta$ a learning rate constant, $\hat{u}(t)$ the value of retinal slip at time $t$, $m_j(t)$ the value of the $j$th filter signal at time $t$ and $\langle\rangle$ denotes the expected value of the enclosed quantity over the time period used for training. The value of $\beta$ was adjusted to give rapid learning without instability.

The training input to the system was a head-velocity signal modelled as coloured noise with unit power. The power had its peak value at 0.2 Hz, then varied with increasing frequency $f$ as $1/f$ (as would occur if white-noise head acceleration were integrated to head velocity). For efficiency, weight-update was implemented in batch mode using 5 s batches of head-velocity data. Performance was assessed (i) from the $\hat{u}(t)$ produced by the model, (ii) by applying a step head-position profile to the trained model and (iii) by comparing the learned cerebellar filter with that of the exact compensating filter. The value of the exact filter $C_e$ was calculated by setting

$$Pm = n, \tag{2.5}$$

i.e. when the filter is exact, the head velocity $n$ is exactly balanced by the eye-movement command $m$, so that no retinal slip is caused by head movement. For any value of $C$, $m$ is given by $m = B(Vn + Cm)$, that is

$$m = \frac{BVn}{1 - BC}. \tag{2.6}$$

Combining equations (2.5) and (2.6) gives the equation for the perfect filter $C_e$ as $PBVn/(1 - BC_e) = n$, so that:

$$C_e = \frac{1}{B} - PV. \tag{2.7}$$

### (b) *Variants of the basic system*

After training with the basic system described above, a number of variants were investigated.

(i) *Variants of B*

(i) The integrator pathway was made undergained as well as leaky (equation (2.2), with $G_i$ reduced from 5 to 2.5, $T_i = 0.5$).

(ii) The integrator was made overgained and non-leaky (equation (2.2), with $G_i$ increased from 5 to 7.5, $1/T_i = 0$).

(ii) *Variants of P*

A second-order version of $P$ was used with transfer function $H_p$ given by

$$H_p = \frac{s(s + 1/T_z)}{(s + 1/T_1)(s + 1/T_2)}, \quad (2.8)$$

where $T_1 = 0.37$ s, $T_2 = 0.057$ s and $T_z = 0.2$ s, taken from Stahl's estimate (Stahl 1992, p. 361) of the best-fit two-pole one-zero transfer function (for eye-position from eye-movement command) to the data of Fuchs *et al.* (1988). This plant was combined with a leaky undergained integrator (equation (2.2), with $G_i = 5.05$, $T_i = 0.5$).

(iii) *Delay*

The retinal-slip signal $\hat{u}(t)$ arriving at $C$ was delayed by 100 ms. The system was trained with a first-order plant (equation (2.1)) and a leaky undergained brainstem controller (equation (2.2), with $G_i = 2.5$, $T_i = 0.5$). Subsequently, a variant of the representation described in equation (2.4) was investigated, in which the components $m_k(t)$ were convolved with an 'eligibility trace' $r(t)$. The equation for the eligibility trace was taken from eqns (11) and (12) of Kettner *et al.* (1997):

$$r(t) \propto te^{-(t/t_{peak})}, \quad (2.9)$$

where $t_{peak}$ was set to 0.1 s.

(iv) *Learning rule*

The learning rule was changed from that shown in equation (2.4) to

$$\delta w_j = -\beta\langle m_j(t)\mathrm{sign}[\hat{u}(t)]\rangle \quad (2.10)$$

and used to train an adaptive filter $C$ with a first-order plant (equation (2.1)) and a leaky undergained brainstem controller (equation (2.2), $G_i = 2.5$, $T_i = 0.5$).

(v) *Basis functions*

The different delays used as basis functions for the predictor variable were subsequently replaced by alternative functions. These included sine waves of different frequencies and decaying exponentials of different time constants, as well as basis functions that were orthogonalized with respect to the motor commands themselves. One method of achieving this was by spectral decomposition, in which the motor outputs for a perfectly compensated first-order plant were subjected to principal component analysis. The 100 eigenvectors derived from the analysis were then used as basis functions (Porrill *et al.* 2002). Learning was examined for the second-order plant with a leaky undergained brainstem controller (see § 2b(ii)).

## 3. RESULTS

The effects of training an adaptive controller with the decorrelation algorithm were first investigated for the compensation of a first-order filter, which is an approximation to the plant that, although simple, has nonetheless proved useful in a range of modelling applications (Robinson 1981). The brainstem controller was represented by a leaky integrator, consistent with the effects of floccular lesions on eye-position stability (Zee *et al.* 1981). The behaviour of the system before training is shown in figure 4. Its inaccurate response to coloured-noise head-velocity input (set to 1 deg s$^{-1}$ root-mean-square amplitude) gave rise to retinal slip (figure 4*a*), with predominantly low-frequency (less than 1 Hz) components, as expected from the properties of the brainstem controller. The correlations between past eye-movement commands and current retinal slip are shown in figure 4*c*. Finally, the system's inaccurate response to a head-position step input (figure 4*d*) indicated an inability to maintain eccentric gaze (time constant *ca.* 1 s), similar to that observed after a saccade in animals with floccular lesions (Zee *et al.* 1981).

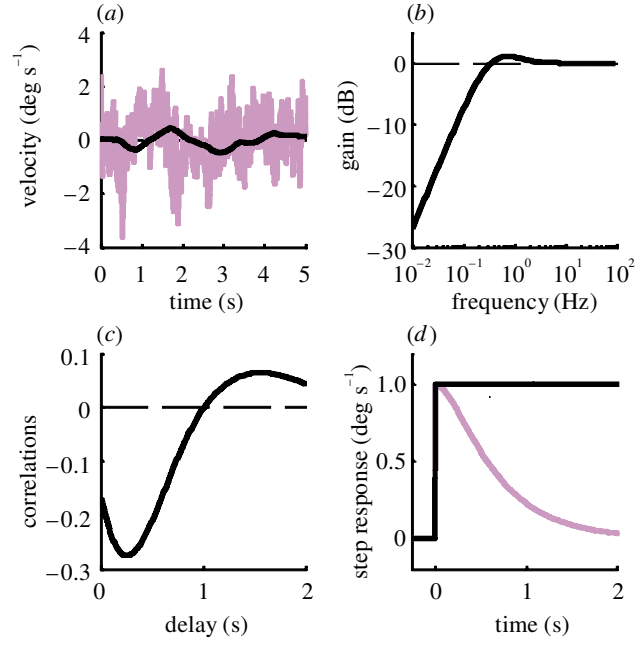


Figure 4. Performance of the model before training, with a first-order plant $P$ (time constant, 0.2 s). The brainstem controller $B$ was a leaky integrator with time constant 0.5 s and accurate high-frequency gain. (*a*) Head velocity (grey line) and retinal slip (solid line). The coloured-noise head-velocity signal (root-mean-square amplitude 1 deg s$^{-1}$) produced a relatively smooth retinal-slip signal. (*b*) The reason for the smoothing is evident from the Bode plot of VOR gain against frequency of head velocity. For frequencies above *ca.* 1 Hz, the VOR gain is close to 1.0 because of the properties of the brainstem controller. (*c*) The correlations present between delayed versions of the eye-movement command and retinal slip, measured over a period of 500 s. (*d*) Eye-position response of the system to a head-velocity pulse (equivalent to head-position step and similar to a saccadic eye-movement command). Grey line, pre; black line, desired. The eye position returns to its initial value with a time course determined by the characteristics of the plant and the brainstem controller.

The effects of training with the decorrelation algorithm are shown in figure 5. A representative time course for training is shown in figure 5*a*. The error was still declining after 1000 trials, but its value at that stage corresponded to little apparent retinal slip (figure 5*b*), to correlations between past commands and current slip indistinguishable from zero (not shown) and eccentric gaze indistinguishable from the 'desired' trace in figure 4*d*. After training, the filter formed by the cerebellar controller $C$ was close to the theoretical ideal (figure 5*c*), which is $B^{-1} - VP$ (derivation in § 2a, equations 2.5–2.7). In short, the decorrelation algorithm was able to learn to compensate

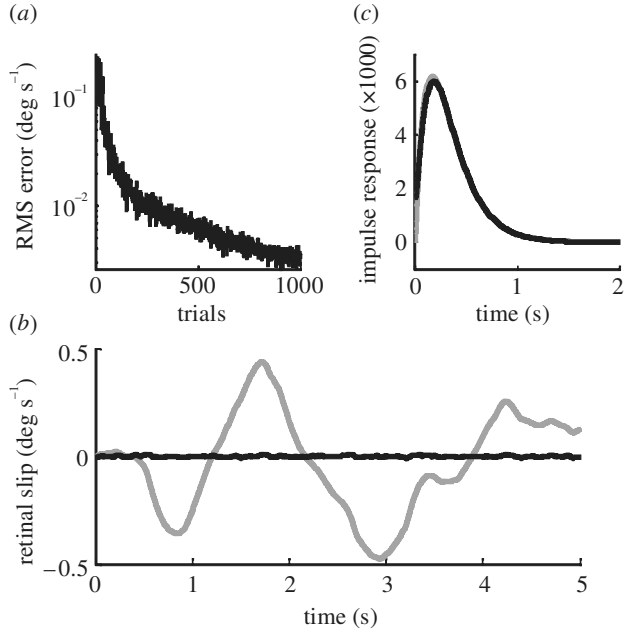


Figure 5. Performance of the model during and after training, with a first-order plant $P$ (time constant, 0.2 s) and a brainstem controller $B$ with a leaky integrator (time constant 0.5 s) and accurate high-frequency gain. (*a*) Typical decline in retinal-slip amplitude with training. Root-mean-square (RMS) retinal-slip amplitude, measured over a 5 s training trial as shown in figure 4*b*, plotted on a log scale against number of training trials. (*b*) The impulse response of the trained decorrelator $C$, compared with that of the ideal filter $C_e$ (grey line, pre; black line, post). (*c*) Post-training reduction in retinal slip (grey line, desired; black line, post) (note the change in scale from figure 4*a*).

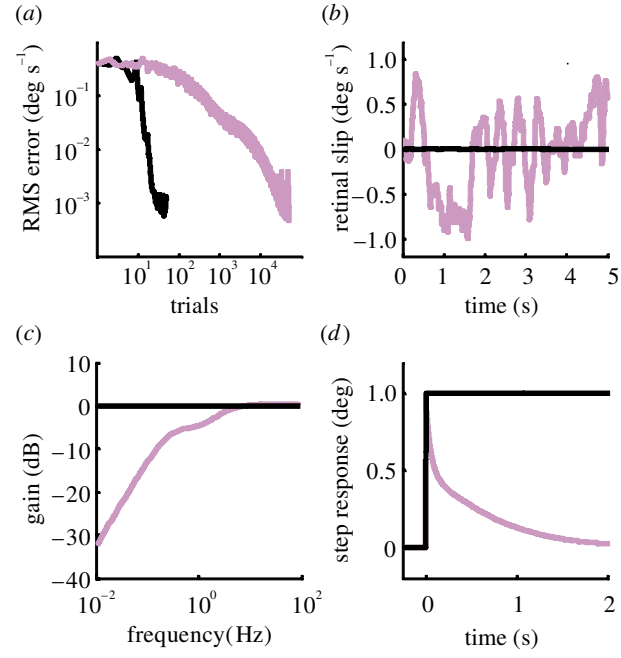


Figure 6. The decorrelation-control algorithm used with a second-order plant $P$ and a leaky-integrator brainstem controller $B$. (*a*) Learning as measured by reduction on root mean square (RMS) retinal-slip amplitude. Note the log scale on both axes. The two curves are for decorrelators with either the 'delay' (grey line) or the 'spectral' (black line) set of basis functions. The latter were an orthogonal set derived from the principal components of compensated motor commands. The final performance of the trained filter was little affected by the basis functions used. (*b*) Pre- (grey line) and post- (black line) training retinal slip in response to a coloured-noise head-velocity input. (*c*) Pre- (grey line) and post- (black line) training Bode gains for the VOR. (*d*) Pre- (grey line) and post- (black line) training eye-position response to a head-velocity pulse.

accurately for a first-order plant, given a leaky brainstem controller.

To establish the robustness of the decorrelation algorithm, we investigated learning with variants of the above basic system (see § 2b).

(i) The precise nature of the brainstem controller $B$ has not been completely specified. The two additional variants tested here were (1) the integrator pathway in $B$ was undergained as well as leaky, and (2) the integrator pathway was overgained, a possible interpretation of data obtained from single-unit recording in rabbits (De Zeeuw *et al.* 1995). In both cases, learning by the decorrelation algorithm was slower than that shown in figure 5*a* (error after 1000 trials *ca.* 4 times larger), but eventual convergence to the ideal filter (not shown) was as good and produced a similar post-training step response to that shown, as the black line ('desired') in figure 4*d*. Convergence was also seen even if the gain of the integrator pathway was set to zero.

(ii) The linearized models that have been proposed for the plant $P$ range from first-order, as used for the results shown in figures 4 and 5, to third- or higher-order. Models made higher-order by inclusion of the inertia of the globe are not relevant to the present study because, in the VOR, the inertia of the globe is acted on by both eye-muscle force and head force and so does not affect the transfer function of eye-movement command to eye-in-world velocity. With inertia excluded, the most frequently used linear models relating eye-movement command to eye position have been second order with two poles and one zero (2P1Z; corresponding to two Voigt elements in series where a Voigt element is a viscosity and elasticity in parallel (e.g. Optican & Miles 1985; Optican *et al.* 1986; Fuchs *et al.* 1988; Stahl 1992; Goldstein & Reinecke 1994)). Accordingly, the decorrelation algorithm was tested with a two-pole one-zero model using the time constants estimated by Stahl (1992) to fit the data of Fuchs *et al.* (1988), and a brainstem controller $B$ that was undergained and leaky. The pre- and post-training performance of the system is shown in figure 6*b–d*, and the learning curve in figure 6*a* (marked 'delay'). Learning by the decorrelation algorithm was slower than that shown in figure 5*a* for the first-order plant, but again eventual convergence to the ideal filter was good (not shown) with near-elimination of retinal slip (figure 6*b*), Bode gains close to 1.0 (figure 6*c*) and an eye-position step response close to the desired value (figure 6*d*).

(iii) The retinal-slip signal that is delivered as climbing-fibre input to the cerebellar flocculus is delayed by about 100 ms (Miles 1991). A delay of 100 ms was

therefore introduced in the model between the generation of the signal $\hat{u}(t)$ and its arrival at the cerebellum $C$. The results of training with a first-order plant and the brainstem controller with an undergained leaky integrator pathway indicated that frequencies in the training data higher than *ca.* 2.5 Hz could cause instabilities. These instabilities were obviated by use of an 'eligibility trace' (see § 2b(iii)), with resultant learning similar to that illustrated in figure 5. The eligibility trace acts in effect as a delay and a smoothing filter to remove high frequencies from the predictor-variable components $m_k(t)$. Its existence is suggested both by behavioural studies of the VOR (Raymond & Lisberger 1998) and by measurements of calcium dynamics in Purkinje cell dendrites (Wang *et al.* 2000).

(iv) The capacity of the climbing-fibre pathway to convey detailed information appears to be limited by low ($< 10$ Hz) firing rates. The decorrelation-control algorithm was therefore tested with a learning rule that simply used the sign of $\hat{u}(t)$, i.e. the direction of retinal slip (see § 2b(iv)). Learning was very similar to that shown in figure 5, except that final performance needed to be improved slightly by reducing the learning rate near to convergence.

(v) Little is known about the actual function of the granule-cell–Golgi-cell complex, here supposed to correspond to the decomposition of the input signal $m(t)$ into components $m_1(t)$, …, $m_n(t)$. Different methods of effecting this decomposition were therefore investigated, including obvious candidates such as sine wave and decaying exponentials. Choice of basis function appeared to influence speed of learning, rather than final convergence. For example, learning the second-order problem (§ 2b(ii)) could be speeded by up to 1000-fold by appropriate choice of basis function, i.e. one that made the components $m_1(t),\ldots,m_n(t)$ orthogonal (figure 6*a*, black line).

## 4. DISCUSSION

We tested decorrelation control, a candidate algorithm for cerebellar function, in a linearized model of oculomotor plant compensation in the VOR. The algorithm proved successful and robust. It was able to decorrelate the predictor variable of eye-movement command from the target variable of retinal slip, both being signals that are available to the cerebellum. The algorithm did not require the unavailable signal of motor error (§ 1 and Appendix A), nor did it depend on any specific decomposition of the predictor variable (such as tapped delay lines).

The proposed application of decorrelation control to oculomotor plant compensation is consistent with evidence concerning the functions of the cerebellar flocculus (e.g. Zee *et al.* 1981; Optican & Miles 1985; Optican *et al.* 1986). Moreover, electrophysiological recordings from Purkinje cells in the primate flocculus indicate that a subset of them carry an eye-position signal, as required by the present model (Lisberger & Fuchs 1978; Noda & Suzuki 1979; Belton & McCrea 2000; Leung *et al.* 2000). Decorrelation control is also consistent with theoretical developments of the basic Marr–Albus–Ito model for cerebellar cortex as an adaptive linear filter (Gilbert 1974; Fujita 1982*a*) and with Sejnowski's covariance rule (Sejnowski 1977; Koch 1999), which is widely used in adaptive-filter type models of both cerebellum (e.g. Gluck *et al.* 1990; Kettner *et al.* 1997; Medina & Mauk 2000) and cerebellar precursors (Roberts & Bell 2000). Decorrelation control shows how these components can be incorporated into a system for motor learning that utilizes only sensory signals.

As well as its power and plausibility in the context of oculomotor plant compensation, decorrelation control provides an alternative to the existing method of avoiding the unavailable signal of motor error, namely feedback error learning (Kawato 1990; Gomi & Kawato 1993). In feedback error learning, an estimate of the motor error ($P^{-1}\hat{u}(t)$, see Appendix A) is provided by the output of a conventional feedback controller, which uses a reference model of the plant and receives the 'sensory error' $\hat{u}(t)$ as input. Decorrelation control has a distinct advantage over feedback error learning in that it does not raise the 'interesting and challenging theoretical problem of setting an appropriate inverse reference model' (Gomi & Kawato 1992, p. 112) . In the specific case of the oculomotor plant, the feedback controller corresponds to the brainstem circuitry used in the optokinetic response (OKR) (Fujita 1982*b*; Gomi & Kawato 1992). It is difficult to compare the present results for compensation of the oculomotor plant directly with those obtained from feedback error learning (Gomi & Kawato 1992). In the latter study, the simulated plant–compensation occurred simultaneously with adaptation of the VOR and OKR, and the basic architecture of the model system did not include the neural integrator in the lower reflex arc, so that 'the flocculus tried to construct its substitute unnaturally' (Gomi & Kawato 1992, p. 110). It is possible that in practice a blend of decorrelation control and feedback error learning is used, exploiting redundancy to decrease the chances of catastrophic failure.

Finally, there is the question of the possible generality of the decorrelation-control algorithm.

(i) For plant compensation itself, preliminary mathematical analysis indicates that, with plausible brainstem filters, decorrelation control is stable in the multidimensional linear case, i.e. it will learn to compensate for any linear plant, provided that the system is configured as in figure 2*b* with a copy of the motor command fed back to the decorrelator (Porrill *et al.* 2002). This analysis also indicates that, under these circumstances, decorrelation control is also applicable to nonlinear systems if a sufficiently rich set of predictor variables is available (for example, containing the nonlinear signal combinations required in a Volterra expansion of the solution). In effect, decorrelation control is a procedure whereby the cerebellum and its associated brainstem (or spinal cord) controller can form an inverse model of the plant (Wolpert *et al.* 1998), using only sensory climbing-fibre input (Simpson *et al.* 1996) to do so. Higher-level controllers, for example in cerebral cortex, are thus enabled to ignore plant characteristics and merely issue simplified commands (such as the desired velocity command already mentioned). This can be seen as a part

of a function long proposed for the cerebellum: 'the purpose of the cerebellum is to learn motor skills, so that when they have been learnt a simple or incomplete message from the cerebrum will suffice to provoke their execution' (Marr 1969, p. 438).

With respect to the feedback configuration shown in figure 2*b*, anatomical tracing of projections from the cerebral cortex to cerebellar cortex (via the pons), and in the opposite direction from cerebellar to cerebral cortex (via the thalamus) indicate that, for a given area of cerebral cortex, the two sets of connections form a loop: 'closed loop circuits may be a fundamental feature of cerebellar interactions with the cerebral cortex' (Middleton & Strick 2000, p. 240). This anatomical evidence is at least consistent with the possibility that the feedback arrangement required by decorrelation control for plant compensation is widespread.

(ii) Achieving plant compensation allows further uses of decorrelation control. In the case of the VOR, one such use would be to correct inadequacies of head-velocity processing (i.e. if $V$ in figure 2*b* ceases to be equal to unity), a procedure known as adaptive inversion (Widrow & Stearns 1985) that would be of relevance to VOR adaptation. Also, it is known that the retinal-slip signal $\hat{u}(t)$ is fed back to the flocculus as a predictor variable (mossy-fibre input) as well as the target variable (climbing-fibre input). Once the plant is compensated, the decorrelation-control algorithm should be able to move the eyes in order to remove any correlations there may be between earlier and later parts of the external signal $u(t)$ itself. This is in effect a mechanism that learns to predict future values of the signal (at least over a time range of the order of 1 s). A mechanism of this kind has been identified in smooth pursuit (e.g. Barnes 1991) and appears to be implemented by the cerebellar flocculus (Kettner *et al.* 1997; Suh *et al.* 2000).

(iii) One of the functions of decorrelation control is to generate an estimate of the target variable that is not predictable by information available to the controller. This estimate is likely to be of use for the acquisition of sensory information during active exploration (e.g. Blakemore *et al.* 2000; Hartmann & Bower 2001). It is this aspect of decorrelation control that serves to reconcile sensory and motor functions of the cerebellum (cf. § 1).

In summary, decorrelation control is a simple, compact and powerful algorithm, well suited to the role of the cerebellum in simplifying both motor control and sensory acquisition in order to liberate computational power at higher levels of the system.

Support for this work was provided by the Biotechnology and Biological Sciences Research Council (BBSRC). J.V.S. was the recipient of a Wellcome mathematical biology fellowship.

## APPENDIX A

In the simplest case of interference cancellation (figure 1*a*), the output of the decorrelator at time $t$ is the value of a single predictor variable $p(t)$ weighted by $w$. For cerebellar-like structures, this output is in fact an estimate of the interference $\hat{n}(t)$ with the sign reversed (see § 1) so that

$$\hat{n}(t) = -wp(t). \tag{A 1}$$

For adaptive interference cancellation, the decorrelator is required to learn the value of the weight $w$ that gives the best estimate of the signal $\hat{u}(t)$, which is equivalent to producing an estimate of interference $\hat{n}(t)$ that is as close to the actual interference $n(t)$ as possible. The error of the estimate at time $t$ is

$$e(t) = n(t) - \hat{n}(t), \tag{A 2}$$

so that the best least-squares estimate of the signal is one that minimizes the sum of squared errors $E$ defined as

$$E = \frac{1}{2}\sum e(t)^2, \tag{A 3}$$

where summation takes place over the time-steps of interest. For the value of $w$ that minimizes $E$, the gradient of the error with respect to the weight $\partial E/\partial w$ is zero. Because by the chain rule $\partial E/\partial w = \partial E \partial e/\partial e \partial w$, and from equations (2.1) and (2.2) $e(t) = n(t) + wp(t)$, then $\partial e/\partial w = p(t)$ and

$$\frac{\partial E}{\partial w} = \sum_t p(t)e(t). \tag{A 4}$$

Therefore when $E$ is at its minimum the quantity $\Sigma_t p(t)e(t)$ is zero. But as this quantity is proportional to the correlation between $p(t)$ and $e(t)$, minimizing $E$ is equivalent to decorrelating $p(t)$ and $e(t)$. This in turn is equivalent to producing a system output $\hat{u}(t)$ that is decorrelated from $p(t)$, because $\hat{u}(t) = u(t) + e(t)$ and the component $u(t)$ is by definition not correlated with $p(t)$.

The desired value of $w$ can be arrived at with the gradient descent learning rule $\delta w = -\beta(E/\partial w)$, where $\delta w$ is the change in the weight and $\beta$ is a learning-rate constant. This rule is also known as the Widrow–Hoff or delta rule (cf. Widrow & Stearns 1985). In the present case,

$$\delta w = -\beta\langle p(t)e(t)\rangle, \tag{A 5}$$

where $\langle p(t)e(t)\rangle$ is the expected value of $p(t)e(t)$ and is proportional to the correlation between $p(t)$ and $e(t)$.

In the case of decorrelation control (figure 1*b*), the output of the decorrelator now has to pass through a plant $P$ in order to provide what is in effect an estimate $\hat{n}(t)$ of the interference $n(t)$. Thus, $\hat{m}(t) = P^{-1}[\hat{n}(t)]$, where $\hat{m}(t)$ is the output of the decorrelator (note the change in notation from figure 1*b*, where this output is called $m(t)$). Producing the best estimate $\hat{n}(t)$ of the interference $n$, requires the decorrelator to learn the best motor command $\hat{m}(t)$. This way of looking at the task introduces two new terms, namely $m(t) = P^{-1}[n(t)]$, where $m(t)$ is the motor command that would produce the perfect interference estimate, i.e. the 'desired motor command' for the system, and $e_{\mathrm{m}}(t) = m(t) - \hat{m}(t)$, where $e_{\mathrm{m}}(t)$ is the 'motor error', namely the difference between desired and actual motor commands. Minimizing the sum-of-squared motor errors $E_{\mathrm{m}}$ entails setting the expression

$$\frac{\partial E_{\mathrm{m}}}{\partial w} = \sum_t p(t)P^{-1}[e(t)] \tag{A 6}$$

to zero (cf. equation (A 4)), that is, decorrelating the predictor variable $p(t)$ and the motor error $P^{-1}[e(t)]$. In a feed-forward architecture, the gradient descent learning rule corresponding to equation (A 6) is:

$$\delta w = -\beta\langle p(t)P^{-1}[e(t)]\rangle. \qquad \text{(A 7)}$$

Comparing equation (A 7) with equation (A 5) for adaptive interference–cancellation indicates that whereas in equation (A 5) the two signals to be decorrelated are both available to the system, in the case of decorrelation control equation (A 7) one of the signals to be decorrelated is not available to the system. The motor error $P^{-1}[e(t)]$ requires knowledge of the plant $P$, which by definition in the problem under consideration is unknown to the controller. Conversely, decorrelating $p(t)$ and $e(t)$ as in equation (A 5) is no longer equivalent to minimizing the least-squares error of the interference estimate once there is a plant in the system.

## REFERENCES


Barnes, G. R. 1991 The mechanism of prediction in human smooth pursuit eye movements. *J. Physiol.* **439**, 439–462.

Bell, C., Bodznick, D., Montgomery, J. & Bastian, J. 1997 The generation and subtraction of sensory expectations within cerebellum-like structures. *Brain Behav. Evol.* **50**, 17–31.

Belton, T. & McCrea, R. A. 2000 Role of the cerebellar flocculus region in cancellation of the VOR during passive whole body rotation. *J. Neurophysiol.* **84**, 1599–1613.

Blakemore, S. J., Wolpert, D. & Frith, C. 2000 Why can't you tickle yourself? *Neuroreport* **11**, R11–R16.

Büttner-Ennever, J. A. & Horn, A. K. E. 1996 Pathways from cell groups of the paramedian tracts to the floccular region. In *New directions in vestibular research*, vol. 781 (ed. S. M. Highstein, B. Cohen & J. A. Büttner-Ennever), pp. 532–540. New York Academy of Sciences.

Devor, A. 2000 Is the cerebellum like cerebellar-like structures? *Brain Res. Rev.* **34**, 149–156.

De Zeeuw, C. I., Wylie, D. R., Stahl, J. S. & Simpson, J. I. 1995 Phase relations of Purkinje cells in the rabbit flocculus during compensatory eye movements. *J. Neurophysiol.* **74**, 2051–2064.

Fuchs, A. F., Scudder, C. A. & Kaneko, C. R. S. 1988 Discharge patterns and recruitment order of identified motoneurons and internuclear neurons in the monkey abducens nucleus. *J. Neurophysiol.* **60**, 1874–1895.

Fujita, M. 1982*a* Adaptive filter model of the cerebellum. *Biol. Cybernetics* **45**, 195–206.

Fujita, M. 1982*b* Simulation of adaptive modification of the vestibulo-ocular reflex with an adaptive filter model of the cerebellum. *Biol. Cybernetics* **45**, 207–214.

Fukushima, K. & Kaneko, C. R. S. 1995 Vestibular integrators in the oculomotor system. *Neurosci. Res.* **22**, 249–258.

Gilbert, P. F. C. 1974 A theory of memory that explains the function and structure of the cerebellum. *Brain Res.* **70**, 1–8.

Gluck, M. A., Reifsnider, E. S. & Thompson, R. F. 1990 Adaptive signal processing and the cerebellum: models of classical conditioning and VOR adaptation. In *Neuroscience and connectionist theory* (ed. M. A. Gluck & D. E. Rumelhart), pp. 131–185. Hillsdale, NJ: Lawrence Erlbaum.

Goldstein, H. & Reinecke, R. 1994 Clinical applications of oculomotor plant models. In *Contemporary ocular motor and vestibular research: a tribute to David A. Robinson; international meeting, Eibsee 1993* (ed. A. F. Fuchs, T. Brandt, U. Büttner & D. Zee), pp. 10–17. Stuttgart, Germany: Georg Thieme.

Gomi, H. & Kawato, M. 1992 Adaptive feedback control models of the vestibulocerebellum and spinocerebellum. *Biol. Cybernetics* **68**, 105–114.

Gomi, H. & Kawato, M. 1993 Neural network control for a closed-loop system using feedback-error-learning. *Neural Networks* **6**, 933–946.

Goodwin, M. M. 1998 *Adaptive signal models: theory, algorithms, audio applications*. Boston, MA: Kluwer.

Hartmann, M. J. & Bower, J. M. 2001 Tactile responses in the granule cell layer of cerebellar folium Crus IIa of freely behaving rats. *J. Neurosci.* **21**, 3549–3563.

Ito, M. 1970 Neurophysiological aspects of the cerebellar motor control system. *Int. J. Neurol.* (*Montevideo*) **7**, 162–176.

Ito, M. 1984 *The cerebellum and neural control*. New York: Raven Press.

Kawato, M. 1990 Feedback-error-learning neural network for supervised motor learning. In *Advanced neural computers* (ed. R. Eckmiller), pp. 365–372. Amsterdam: Elsevier.

Kettner, R. E., Mahamud, S., Leung, H. C., Sitkoff, N., Houk, J. C., Peterson, B. W. & Barto, A. G. 1997 Prediction of complex two-dimensional trajectories by a cerebellar model of smooth pursuit eye movement. *J. Neurophysiol.* **77**, 2115–2130.

Koch, C. 1999 *Biophysics of computation*. Oxford University Press.

Leung, H.-C., Suh, M. & Kettner, R. E. 2000 Cerebellar flocculus and paraflocculus Purkinje cell activity during circular pursuit in monkey. *J. Neurophysiol.* **83**, 13–30.

Lisberger, S. G. 1998 Physiologic basis for motor learning in the vestibulo-ocular reflex. *Otolaryngol. Head Neck Surg.* **119**, 43–48.

Lisberger, S. G. & Fuchs, A. F. 1978 Role of primate flocculus during rapid behavioral modification of vestibuloocular reflex. I. Purkinje cell activity during visually guided horizontal smooth-pursuit eye movements and passive head rotation. *J. Neurophysiol.* **41**, 733–763.

Marr, D. 1969 A theory of cerebellar cortex. *J. Physiol.* **202**, 437–470.

Medina, J. F. & Mauk, M. D. 2000 Computer simulation of cerebellar information processing. *Nature Neurosci.* **3**, 1205–1211.

Middleton, F. A. & Strick, P. L. 2000 Basal ganglia and cerebellar loops: motor and cognitive circuits. *Brain Res. Rev.* **31**, 236–250.

Miles, F. A. 1991 The cerebellum. In *Eye movements* (ed. R. H. S. Carpenter), pp. 224–243. Basingstoke, UK: MacMillan.

Nakamagoe, K., Iwamoto, Y. & Yoshida, K. 2000 Evidence for brainstem structures participating in oculomotor integration. *Science* **288**, 857–859.

Nelson, M. E. & Paulin, M. G. 1995 Neural simulations of adaptive reafference suppression in the elasmobranch electrosensory system. *J. Comp. Physiol.* A **177**, 723–736.

Nixon, P. D. & Passingham, R. E. 2001 Predicting sensory events: the role of the cerebellum in motor learning. *Exp. Brain Res.* **138**, 251–257.

Noda, H. & Suzuki, D. A. 1979 The role of the flocculus of the monkey in fixation and smooth pursuit eye movements. *J. Physiol.* **294**, 335–348.

Optican, L. M. & Miles, F. A. 1985 Visually induced adaptive changes in primate saccadic oculomotor control signals. *J. Neurophysiol.* **54**, 940–958.

Optican, L. M., Zee, D. S. & Miles, F. A. 1986 Floccular lesions abolish adaptive control of post-saccadic ocular drift in primates. *Exp. Brain Res.* **64**, 596–598.

Paulin, M. G. 1993 The role of the cerebellum in motor control and perception. *Brain Behav. Evol.* **41**, 39–50.

Porrill, J., Dean, P. & Stone, J. V. 2002 A cerebellar architecture for adaptive plant compensation. (In preparation.)

Raymond, J. L. & Lisberger, S. G. 1998 Neural learning rules for the vestibulo-ocular reflex. *J. Neurosci.* **18**, 9112–9129.

Roberts, P. D. & Bell, C. C. 2000 Computational consequences of temporally asymmetric learning rules: II. Sensory image cancellation. *J. Comput. Neurosci.* **9**, 67–83.

Robinson, D. A. 1975 Oculomotor control signals. In *Basic mechanisms of ocular motility and their clinical implications* (ed. G. Lennerstrand & P. Bach-y-Rita), pp. 337–374. Oxford: Pergamon.

Robinson, D. A. 1981 Models of the mechanics of eye movements. In *Models of oculomotor behaviour* (ed. B. L. Zuber), pp. 21–41. Boca Raton, FL: CRC Press.

Sejnowski, T. J. 1977 Storing covariance with nonlinearly interacting neurons. *J. Math. Biol.* **4**, 303–321.

Simpson, J. I., Wylie, D. R. & De Zeeuw, C. I. 1996 On climbing fiber signals and their consequence(s). *Behav. Brain Sci.* **19**, 384–398.

Stahl, J. S. 1992 Signal processing in the vestibulo-ocular reflex of the rabbit. PhD thesis. New York University.

Suh, M., Leung, H. C. & Kettner, R. E. 2000 Cerebellar flocculus and ventral paraflocculus purkinje cell activity during predictive and visually driven pursuit in the monkey. *J. Neurophysiol.* **84**, 1835–1850.

Wang, S. S.-H., Denk, W. & Häusser, M. 2000 Coincidence detection in single dendritic spines mediated by calcium release. *Nature Neurosci.* **3**, 1266–1273.

Widrow, B. & Stearns, S. D. 1985 *Adaptive signal processing*. Engelwood Cliffs, NJ: Prentice-Hall.

Wolpert, D. M., Miall, R. C. & Kawato, M. 1998 Internal models in the cerebellum. *Trends Cogn. Sci.* **2**, 338–347.

Zee, D. S., Yamazaki, A., Butler, P. H. & Gücer, G. 1981 Effects of ablation of flocculus and paraflocculus on eye movements in primates. *J. Neurophysiol.* **46**, 878–899.

As this paper exceeds the maximum length normally permitted, the authors have agreed to contribute to production costs.